Engineering Conferences International
ECI Digital Archives

5th International Conference on Porous Media and Their Applications in Science, Engineering and Industry

Refereed Proceedings

Summer 6-27-2014

Use of liquid pressure-pulse decay permeameter in experimental evaluation of permeability in wellbore cement under geopressured geothermal conditions

Kolawole Bello
Craft and Hawkins Department of Petroleum Engineering, Louisiana State University

Mileva Radonjic
Craft and Hawkins Department of Petroleum Engineering, Louisiana State University

Proceedings of the 5th International Conference on Porous Media and its Applications in Science and Engineering
ICPM5
June 22-27, 2014, Kona, Hawaii

USE OF LIQUID PRESSURE-PULSE DECAY PERMEAMETER IN EXPERIMENTAL EVALUATION OF PERMEABILITY IN WELLBORE CEMENT UNDER GEOPRESSURED GEOTHERMAL CONDITIONS

Kolawole S. Bello and Mileva Radonjic
Craft and Hawkins Department of Petroleum Engineering, Louisiana State University, Baton Rouge, Louisiana, U.S.A.

ABSTRACT
Geopressured reservoirs in the northern Gulf of Mexico basin along the coast of Louisiana have been determined to be viable source of geothermal energy and potential sites for carbon sequestration, where CO_2 can be utilized to induce convective flow of geofluids and enhance heat harvesting. These reservoirs are made of unconsolidated sandstone capped by shale layers and possess temperatures as high as 140^0C. At high temperatures, cement strength retrogression occur when calcium silicate hydrate phase in hydrated cement converts to alpha dicalcium silicate hydrate phase. The higher the temperature, the quicker the rate of transformation of calcium silicate hydrate. The conversion changes the structure of the hydrated cement leading to increased porosity, permeability and lowered compressive strength. The real problem lies in the great increase of permeability which makes the cement susceptible to chemical attack by low pH formation fluids which lead to loss of hydraulic barrier capability of cement, the most important function of cement in well bore system. The consequence of the loss of zonal isolation is the environmental release of previously contained geofluids,
This study uses liquid pressure-pulse decay permeameter (PDPL) to measure the effect of increased temperature on cement permeability. PDPL is computer operated device capable of measuring permeability of cement to liquid (water) under reservoir conditions. Compared to conventional (steady state) methods, the liquid pressure-pulse decay permeameter cuts down the long time required to stabilize water fluxes from days or weeks to hours. This is very critical as cement permeability could change due to leaching or hydration during the time required in steady state methods. Permeability is calculated using pressure decay across a cement core sample over time. For the experiment, a range of chemical additive were added to portland cement slurry to counteract and curb strength retrogression, changing cement hydration products into chemically more stable phases, with favorable Ca to Si ratio. Four 13.1 pounds per gallon (ppg) (with water to solid ratio of 0.87) cement slurry designs with silica flour, calcined clay, silica sand, steel fiber and glass fiber and 13.1 ppg neat cement slurry were subjected to cycle thermal loading in salt brine. The results indicates that glass fiber and steel fiber cement can be added to the design to improve the permeability and increase the strength of the cement sheath for geopressured geothermal reservoirs in the Gulf of Mexico.

1 INTRODUCTION
Geothermal systems serve as ample source of sustainable carbon-free energy used in the generation of electricity, space heating and air conditioning. Geopressured aquifers, a type of geothermal systems are undercompacted brine saturated porous and permeable formations that have anomalously high pore pressures and temperatures. In the Gulf of Mexico, geopressured reservoirs form as a result of rapid sediment loading from riverborne systems and their deltas. The penetration of sands into underlying muds resulted in isolation of large sand members from the overlying strata. The weight of the sediment layer on the trapped fluids results in elevated pore pressures. These isolated units of sands and muds contain pore pressure of 15.269 kPa/m (0.675psi/ft.), or higher [1]. In addition, expulsion of water into sands from underlying shale as montmorillite converts to illite contributes to the elevated pressure [2]. Temperatures in geopressured reservoir typically range from 90^0C to $200+^0$C with salinities as high as 100 g/L [3]. Camerina Sand A, a geopressured geothermal reservoir in Vermilion Parish, Louisiana [4] is used as a case study. The main concern with producing these geopressured reservoirs pertains to the environmental changes brought about by the removal of vast amounts of high-pressure, subsurface water and the subsequent decrease in reservoir pressures. This can result in surface subsidence or worse induce an earthquake [5]. Novel wellbore system with downhole heat exchanger is been

investigated for in-situ heat harvesting resulting in zero-mass withdrawal [6].

Drilling and completing high temperature wellbores are always a challenge due to the durability of materials and downhole assembly including wellbore cements. Portland cement is the main component used in wellbore cement slurries. It is used for primary cementing, wellbore remediation and plug and abandonment of wells. Hardened cement is formed by mixing unhydrated cement clinker with water. Upon complete hydration, the two main hydration products are: calcium silicate hydrate and calcium hydroxide. The concentration of the mineral phases in the unhydrated cement as well as the hydration temperature determines the rate of hydration, the strength and the permeability of hydrated product. The degree of hydration of cements with water to cement ratio between 0.3 and 0.6 does not change substantially after 28 days at ambient conditions [7]. This point can be achieved in less number of days at higher temperature. Calcium silicate hydrate is the main binding phase and thus influences strength in hydrated cement [8]. Cement is a porous material with highly alkaline (pH~13) pore solution (pore water), depending on the water to cement ratio. The alkalinity maintains the calcium hydroxide in the cement matrix. The higher the degree of hydration, the lower the porosity and permeability as calcium hydroxide converts to calcium silicate hydrate.

The most important purpose of cementing is zonal isolation. Failures in cement sheaths can lead to the contamination of fresh water aquifer, migration of reservoir fluids from high pressure sands to low pressure sands and sustained casing pressure as a result of fluid migration from the reservoir to the surface. Production and injection of geofluids in proposed geothermal well will result in thermal loading of the cement possibly causing failure within the cement sheaths and interface de-bonding. This changes the structure of the hydrated cement leading to increased porosity, permeability and lowered compressive strength [9]. The real problem lies in the great increase of permeability as it makes the cement susceptible to corrosive formation fluids [10]. Experimental studies by Yalkinkaya et al. shows that exposure of cement fracture to CO_2 rich brine will increase the porosity and widen the fracture [11].

2. EXPERIMENTAL MATERIALS AND PROCEDURE

To study the behavior of cement in proposed wellbore [6], a batch experiment was conducted using 4 different class H cement slurry design (Table 1.) Four 13.1 pounds per gallon (ppg) (1.31 g/cc) cement slurry designs with cement additives to accommodate for the severe environmental conditions were investigated and compared with 13.1 ppg neat cement slurry. All four cement slurry designs contain class H cement and silica flour. Fine metakaolin, silica sand, steel fiber and polymer were added to the first, second, third and fourth sample respectively (Table 1). The calcined clay has a grain size ranging from 45 microns to 75 microns. The calcined clay and steel fiber have a size range of 5 microns and 400 microns respectively. The glass fiber has the biggest grain size of the additives with a range of 3-5mm. The chemical additives were added to Portland cement slurry to counteract and curb strength retrogression, by changing cement hydration products into chemically more stable phases, with favorable Ca to Si ratio. The selected additives were also chosen because of their potential to prevent thermal micro fracturing of cement sheath. Cement core samples were made according to the American Petroleum Institute (API) recommended practice [12].

Table 1: Mix proportions of cements by mass.

Design	Neat Cement	Steel Fiber Cement	Silica Sand Cement	Calcined Clay Cement	Glass Fiber Cement
Class H Cement	1	1	1	1	1
Bentonite	0.02	0.02	0.02	0.02	0.02
Silica Flour	-	0.35	0.35	0.35	0.35
Steel Fiber	-	0.02	-	-	-
Silica Sand	-	-	0.02	-	-
Calcined Clay	-	-	-	0.02	-
Glass Fiber	-	-	-	-	0.02
Water	0.87	1.17	1.17	1.17	1.17

The cement slurry was prepared by mixing Class H cement and distilled water at a water to solid ratio ratio of 0.87. The mixing was done with a four liter, 3.75 horsepower Waring® blender. Bentonite and water was mixed first at 16,000 revolutions per minute (RPM). After 5 minute, the rest of the material was added to the mixture in the blender and mixed at 20,000 RPM for the next 35 seconds. The cement slurry was poured into 3 in. X 1 in. cylindrical brass molds. The wait on cement period was 24 hours after which the cement cores were de-molded and used in the experiments.

Hydrated cement cores were subjected to cycles of differential temperature of $50^{o}C$ with 100% relative humidity (RH) in experimental brine (Table 2) in temperature cycling/relative humidity (environmental) chamber. Each cycle took 12 hours with the temperature ramped from $40^{o}C$ to $90^{o}C$ and back to $40^{o}C$. The environmental chamber is an ESPEC EGNL12-4CAL model with a lower and upper temperature limit of $-40^{o}C$ and $180^{o}C$ respectively. The experiment was limited by the boiling point of water, and that was why it was conducted at $90^{o}C$ rather than over $100^{o}C$ as reported in literature.

Table 2: Brine Composition for Experiments. The brine was designed to simulate the fluid composition of Camerina sand.

Salts	Amount mixed with 1L of distilled water
Sodium Chloride (NaCl)	32.19 g
Potassium Chloride (KCl)	0.454 g
Magnesium Chloride ($MgCl_2$)	0.991 g

The porosity, density, permeability and compressive strengths of the samples were taken after 100 cycles. The porosity and density was measured using a Ultragrain Grain Volume Porosimeter, UGV-200 from Core Laboraties. The UGV-200 utilizes Boyles Law helium gas expansion porosimetry. 10 cc of helium gas at a certain pressure is expanded into the cement cores. The final pressure occupied by the gas is then used to determine the grain volume of the cement cores. The grain volume with the bulk volume of the core is then used to determine the porosity of the cement cores. The grain volume and the weight of the cores are also used to determine the density of the hydrated cement cores. The bulk volumes of the cores were calculated from the core dimensions taken with a caliper while the weight of the cores are measured using a mass balance.

Laboratory measurement of low permeability media such as cement to water is usually a technical challenge. A liquid pressure-pulse decay permeameter model CFS-200 was used to determine the permeability of the cement cores as it employs a transient technique to measure cement permeability to water. Cores are placed in a pressure vessel that allows hydrostatic confining pressures as high as 680 bar (10000 psi), maximum back pressure of 400 bar (6000 psi) and resist temperatures to ~ 150^{0}C. The permeability is a function of pressure decay through the core over time using semilog analysis [13,14]. The permeability was reported in nanoDarcy (nD) (equivalent to 10^{-21} m^2).

Compared to conventional (steady state) methods, the liquid pressure-pulse decay permeameter cuts down the long time required to stabilize water fluxes from days or weeks to hours. This is very critical as cement permeability could change due to leaching or hydration during the time required in steady state methods [15,16].

A Model 4207D Compressive Strength Testers would be used to measure the unconfined maximum compressive strength of hydrated cement cores after 100 thermal cycles according to the API RP 10A [12]. This was done in order to quantify the effect of thermal cycle loading on the strength of the cement.

3 RESULTS

3.1 Cement Porosity

Porosity was determined on two cores from each sample design using a Helium Boyle's Law Porosimeter. The cores were approximately 5.08 cm. (2 in.) length and 2.54 cm. (1 in.) in diameter. Table 3 summarizes the porosity of the four designs after 100 cycles. Steel cement design exhibit the least porosity with an average of 53.64 %. The highest porosity average was 57.61% measured in glass fiber cement cores. Figure 1 displays the density and the porosity of the cement cores. A cement core containing glass fiber had the highest porosity at 58.34% while a cement core containing steel fiber had the least porosity of 51.03%. It should be noted that the density of the steel cement core with the least porosity was smaller compared to the rest of the cores. The porosities of the all the cores were very similar with a range of 7.31% and a smaller range of 2.98% if the 51.03% porosity measured in one the steel fiber samples was not considered.

Table 3: Average density and average porosity of cement sample designs. Glass fiber cement design had the highest porosity while steel fiber cement design possessed the least porosity.

Cement Design	Average Density [g/cc]	Average Porosity [%]
Neat Cement	2.343±0.015	57.41±0.608
Steel Fiber	2.334±0.074	53.64±3.691
Silica Sand	2.3923±0.001	56.77±0.332
Calcined Clay	2.381±0.002	55.54±0.255
Glass Fiber	2.377±0.031	57.61±1.039

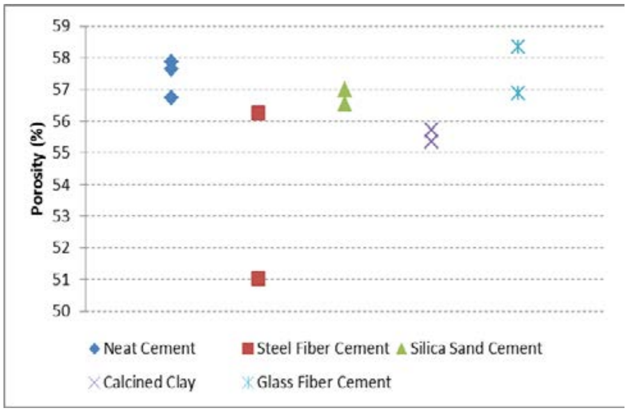

Figure 1: Densities and porosities of cement cores from the thermal cycle loading experiment. The least porosity was measured in a steel cement sample with an anomalous density.

3.2 Cement Permeability

Permeability was carried out on wet cement cores after 100 thermal loading cycles using a liquid pulse pressure decay permeameter. Permeability in all cement designs were close in the 10^{-6} - 10^{-7} D range. Glass fiber cements had the least permeability with an average of 55.72 nD. Silica sand cements had the highest average permeability at 731.4 nD. The neat cement design had a lower permeability compared to the steel fiber cement design and the Table 4 shows the average permeability value of each cement design while Figure 2 displays permeability value for all samples measured.

Table 4: Average permeability of the cement designs after 100 thermal loading cycles. Silica sand cement design exhibit the highest permeability while glass fiber cement design has the least permeability.

Cement Design	Permeability [nD]
Neat Cement	305.2±28.85
Steel Fiber	343.4±97.72
Silica Sand	731.4±116.7
Calcined Clay	289.7±52.06
Glass Fiber	55.72±21.09

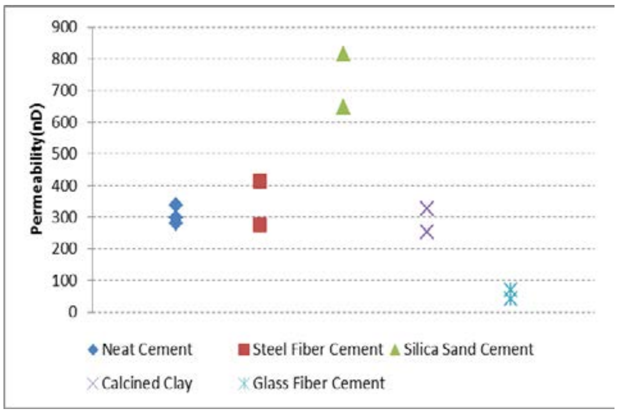

Figure 2: Permeability of each cement sample from all designs after 100 thermal loading cycles. Silica sand cement samples had the highest permeability at approximately 649 nD and 814 nD. Permeability of glass fiber cement samples were the smallest at approximately 71 nD and 41 nD.

3.3 Cement Compressive Strength

The Compressive Strength Tester measures the maximum force required to compress the cement core. The maximum force is divided by the cross sectional area of the cement core to derive the compressive strength. Two cores from each design were tested for strength. A summary of the results is presented in Table 5. Figure 3 displays the maximum force required to breakdown each sample and the calculated compressive strength. The average compressive strength of the cement designs with steel fibers, silica sand, calcined clay and glass fibers are 2.874 MPa [416 psi], 2.138 MPa [310.1psi], 2.656 MPa [385.2 psi] and 1.460 MPa [211.7 psi] respectively.

4. DISCUSSION

The steel cement is the best design regarding porosity. It has 7% less porosity compared to the neat cement. Cores from the silica sand and calcined clay designs have 1% and 3% less porosity respectively with reference to the neat cement. Due to the compactness of the porosity values, it can be said that the effect of the additives on the porosity is insignificant.

The permeability of the glass fiber design was approximately a magnitude of 10nD less than the rest of the cement designs. This is very critical in preventing corrosive alkaline reservoir brine from penetrating into the cement and leaching out Ca out of the cement matrix. The variation in the porosity and permeability values for each design is related to the different microstructure present in the cement sheaths (Figure 6).

The impact of the additives on the cement can be best observed in the compressive strength result. The consistent higher strength measured in the steel fiber design cores indicate they can be used to improve the strength of the cement in the proposed wellbore conditions.

Table 5: Average compressive strength of the cement designs. Cement designs with steel fibers exhibit the most compressive strength while cement designs with glass fibers have the least compressive strength.

Cement Design	Average Compressive Strength [MPa]
Neat Cement	2.822±1.144
Steel Fiber	3.034±0.539
Silica Sand	2.879±1.333
Calcined Clay	2.794±1.081
Glass Fiber	1.989±0.919

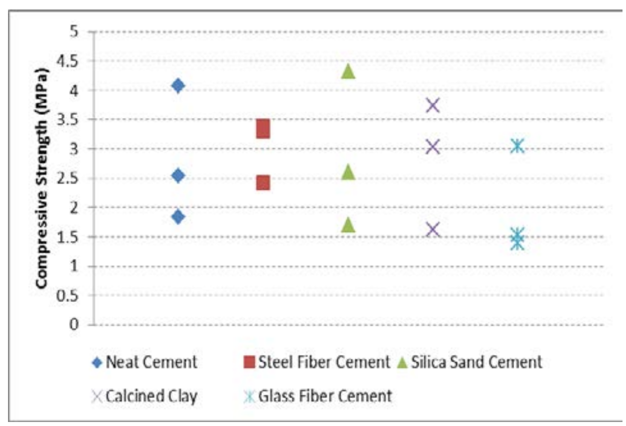

Figure 3: Detailed result Compressive strength of 5.08 cm (2 in.) length and 2.54 cm. (1 in.) diameter cores from the different cement designs. The compressive strength tester measured the maximum compressive force required to breakdown the cores which then divided by the core's surface area to calculate the compressive strength.

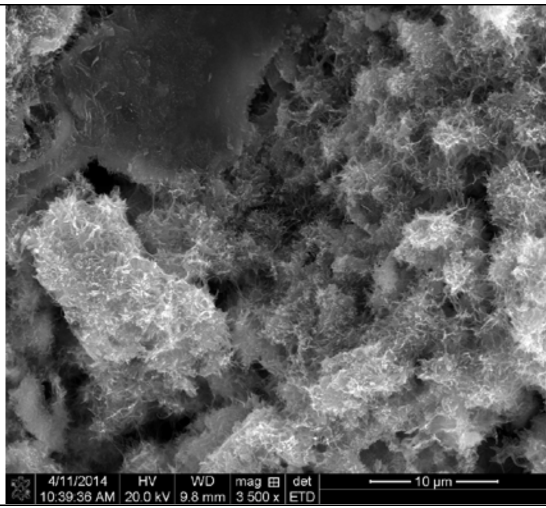

A. SEM image of cement sheath with no additive after 100 thermal loading cycles.

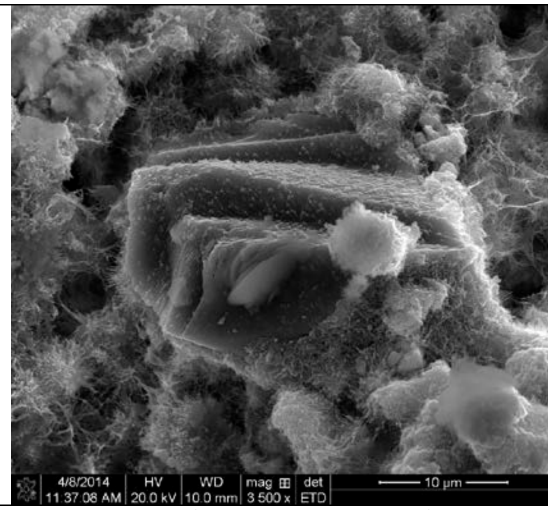

B. SEM image of cement sheath with silica flour and steel fiber after 100 thermal loading cycles.

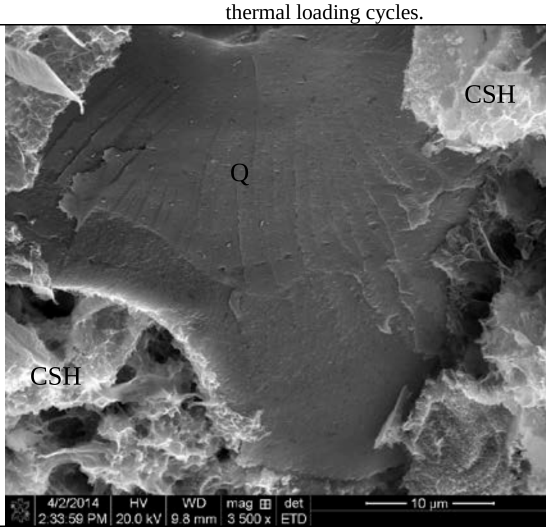

C. SEM image of cement hardened with silica flour and silica sand. Q stands for quartz while CSH is used to represent calcium silicate hydrate gel.

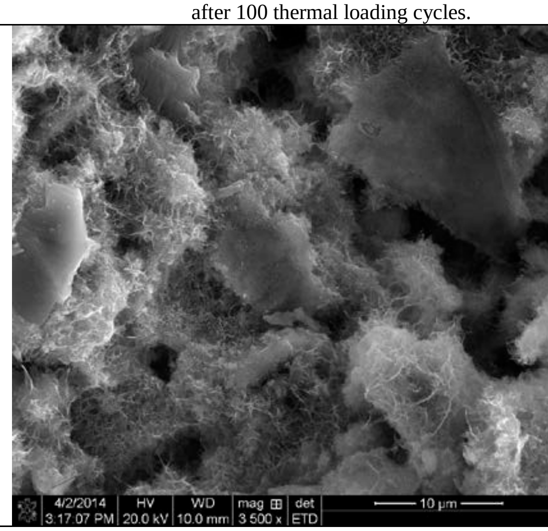

D. SEM image of cement sheath with silica flour and calcined clay after 100 thermal loading cycles.

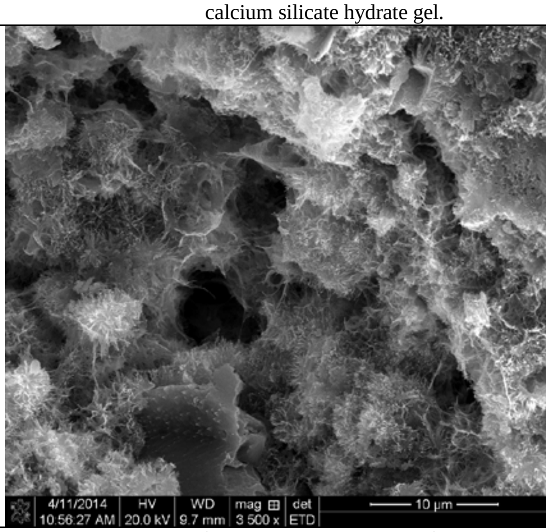

E. SEM image of hardened cement slurry after 100 thermal loading cycles

	Figure 6C Q Composition		Figure 6C CSH Composition	
Element	Weight %	Atomic %	Weight %	Atomic %
C	-	-	2.27	6.10
O	44.81	59.96	24.71	49.92
Al	0.11	0.08	-	-
Si	50.00	38.11	6.01	6.91
Cl	0.42	0.25	4.75	4.33
Ca	2.58	1.38	32.44	26.16
Fe	-	-	3.98	2.30

F. EDS analysis of Figure 6C showing the presence of quartz mineral (Q) and calcium silicate hydrate gel (CSH)

Figure 6: Scanning Electron Microscope (SEM) images of samples from cement design. While the mineral composition is similar in all the cement designs, the microstrure observed is different influencing the poro-mechanical properties. Figure 6F is an example of spatial composition used in confirming minerals observed in SEM images.

5. CONCLUSION

The liquid pressure-pulse decay permeameter provides an accurate, time efficient way to measure cement permeability with the porosity known. Long, uneven fibers such as glass fibers can be used to improve permeability in wellbore cement sheath.

For proposed wellbore in [5], addition of steel fibers and glass fiber along with silica flour would be necessary to increase the durability cement sheath over life of the well.

AKNOWLEDGEMENT

The authors wish to thank the Department of Energy for funding this project. We would also like to express our sincere gratitude to Richard DuBois of Halliburton Drilling Fluids Lab in Broussard, LA for his help with compressive strength measurements and providing us with silica flour, silica sand, steel fiber, and glass fibers. Lastly, we wish to thank Rodney Macon of TXI in Houston, TX for providing us with calcined clay.

REFERENCES

[12] American Petroleum Institute (1977) Recommended practice for testing oil-well cements and cement additives. API Recommended Practice 10.12 ed.

[16] Boulin PF, Bretonnier P, Gland N, Lombard JM (2012) Contributions of the steady state method to water permeability measurement in very low permeability porous media. Oil and Gas Science and Technologies-Rev. IFP Energies nouvelles. 67:387-401.

[14] Chen T, Stagg PW (1984) Semilog analysis of the pulse-decay technique of permeability measurement. Society of Petroleum Engineers. Doi: 10.2118/11818-PA.

[2] Dorfman, M. 1982. The outlook for Geopressured/Geothermal Energy and Associated Natural Gas. In Journal of Petroleum Technology. 34, 9:1915-1919.

[6] Feng Y, Tyagi M., and White CD (2011) Effect of natural convection patterns on optimal location and size of a heat sink in a geothermal reservoir. In proceedings of the 36th Workshop on Geothermal Engineering, Stanford University, Stanford, California.

[1] Griggs J (2004) A Re-Evaluation of Geopressured-Geothermal Aquifers as an Energy Resource. Master's Thesis. Louisiana State University.

[3] Hanor JS, Mercer JA (2010) Spatial variations in the salinity of pore waters in northern deep water Gulf of Mexico sediments: implications for pathways and mechanisms of solute transport. In Geofluids. 10:83-93

[5] Herrin E (1975) Environmental problems associated with the production of energy from geopressured reservoirs, In proceeding of Geopressured Geothermal Energy Conference, Austin, Texas, 2 - 4 June, 1975.

[13] Jones SC (1997) A technique for faster pulse-decay permeability measurements in Tight Rocks. SPE Formation Evaluation.

[4] McCoy RL, Hartsock JH, Dobson RJ (1980) Preliminary results of the wells-of-opportunity geopressured-geothermal testing program. Presented at the SPE/DOE Symposium on Unconventional Gas Recovery, Pittsburgh, Pennsylvania, May 18 - 21, 1980.

[7] Nelson EB, Guillot D (2006) Chemistry and characterization of Portland cement. In Well Cementing. Schlumberger, Houston, Texas.

[15] Scherer GW, Valenza JJ, Simmons G (2006) New methods to measure liquid permeability in porous materials. In Cement and Concrete Research. 37:386-397.

[10] Sugama T (2006) Advanced cements for geothermal wells. Final report prepared for The U.S Department of Energies Office of Geothermal Technologies. Upton, New York: Brookhaven National Laboratory

[9] Taylor HFW (1997) Admixtures and special uses of cement. In Cement Chemistry. Thomas Telford Services, London.

[8] Taylor HFW (1997) Hydration of Portland cement. In Cement Chemistry. Thomas Telford Services, London.

[11] Yalkinkaya T, Radonjic M, Willson CS, and Bachu S (2011) Experimental study on a single cement-fracture using CO_2 rich brine. In Energy Procedia. 4:5335-5342